

## CHAPTER 33

### VERTICAL VARIATION OF UNDERTOW IN THE SURF ZONE

Akio Okayasu<sup>\*</sup>, Tomoya Shibayama<sup>\*\*</sup> and Kiyoshi Horikawa<sup>\*\*\*</sup>  
S.M. JSCE    M. JSCE, A.M. ASCE            M. JSCE, F. ASCE

#### ABSTRACT

In order to establish a model of the vertical distribution of the undertow, laboratory experiments were performed on uniform slopes of 1/20 and 1/30. The turbulent velocity in the surf zone including the area close to the bottom was measured by using a two-component laser doppler velocimeter. The distributions of the mean Reynolds stress and the mean eddy viscosity coefficient were calculated. Based on the experimental results, a model to predict the vertical profile of the undertow was presented.

#### 1. INTRODUCTION

The velocity field in the surf zone is of great importance in the coastal engineering problems. In order to predict the sediment transport rate or the wave attenuation rate in the surf zone, it is necessary to estimate the velocity distribution with high accuracy. Especially, the prediction of the velocity near the bottom is necessary for the evaluation of both of the sediment transport rate and the bottom friction factor. In this study, we focus our attention on the evaluation of the undertow in the inner region of the surf zone.

The existence of the undertow was first observed by Bagnold (1940). After that, some researches of the undertow were carried out with laboratory measurements [see e.g. Hansen and Svendsen (1984)]. Recently, Svendsen (1984) presented a model for estimating the vertical distribution of the undertow applying the eddy viscosity model. He used a boundary condition in which the mass transport velocity on the bottom was given by the Stokes wave theory. Tsuchiya et al.(1988) gave the boundary condition at the trough level.

---

\* Graduate Student, Dept. of Civil Eng., Univ. of Tokyo, Bunkyo-ku, Tokyo, 113 JAPAN

\*\* Associate Professor, Dept. of Civil Eng., Yokohama National Univ., Hodogaya-ku, Yokohama, 240 JAPAN

\*\*\* Professor Emeritus, Univ. of Tokyo; Professor, Dept. of Civil Eng., Saitama Univ., Urawa, Saitama, 338 JAPAN

Okayasu et al.(1986) also presented a model which had a slip condition on the bottom. Nadaoka and Hirose (1986) evaluated the diffusion coefficient in the surf zone. They also discussed the vertical distribution of the steady current on the basis of the distribution of the mean vorticity.

However, the above mentioned studies may have a problem in formulating the velocity field near the bottom, and therefore they may not accurately evaluate the velocity distribution near the bottom or the bottom shear stress. From this point of view, Svendsen (1988) theoretically evolved his model taking the bottom boundary layer into account, but the applicability is still unknown. One reason for that is the lack of the velocity data near the bottom.

In the present study, laboratory experiments on constant slopes were performed under various regular wave conditions. The velocity field in the surf zone including the area close to the bottom was measured by a two-component laser doppler velocimeter. The first objective of the present study is to evaluate the distributions of the mean Reynolds stress and the mean eddy viscosity coefficient in the surf zone based on the experimental results. The second objective is to present a model for estimating the vertical distribution of the steady current below the trough level which is valid through the inner region of the surf zone including near the bottom.

## 2 EXPERIMENT

### 2.1 Experimental Arrangements

Ten experiments were performed on 1/20 and 1/30 constant slopes of smooth beds for various incident waves. The flume was 23m long and 0.8m wide and had a partition at the center for the sake of keeping the phenomena to be two-dimensional. In Case 5, plastic mirrors were placed on the bottom to prevent reflected laser beams from disturbing the signal. This was proved to be successful in getting velocity data with high S/N (signal to noise) ratio. The still water

Table 1 Experimental condition

Case	slope	$T$ (s)	$H_i$ (cm)	$H_0/L_0$	$x_b$ (cm)	$x_p$ (cm)
1		2.00	8.50	0.0139	-270	-220
2		2.00	5.63	0.0092	-200	-165
3	1/20	1.17	9.87	0.0502	-275	spilling
4		0.91	6.69	0.0542	-200	spilling
5		1.50	7.48	0.0230	-250	-200
6		1.61	8.80	0.0232	-410	spilling
7		1.97	6.17	0.0104	-290	-230
8	1/30	1.96	8.22	0.0140	-410	spilling
9		1.12	8.26	0.0457	-350	spilling
10		1.23	6.05	0.0279	-290	spilling

depths in the offshore regions were 40.0cm (39.5cm in Case 5). The experimental condition is listed in Table 1.

In the table,  $T$  is the wave period,  $H_i$  the wave height in the offshore region of the constant depth,  $H_0/L_0$  the deep-water wave steepness,  $x_b$  the wave breaking point,  $x_p$  the wave plunging point. The  $x$ -axis and  $z$ -axis were set to be shoreward and vertically upward, respectively. The origin of the co-ordinates was the shoreline at the still water level.

An arrangement of the measuring points which was rough in the horizontal direction and close in the vertical direction was adopted for the purpose of detailed measurements of the undertow profiles. The measuring points were arranged along 6 or 7 vertical measuring lines in every case except Case 5. The arrangement of Case 5 will be mentioned later. The first measuring line was set on the wave breaking point. The second line was located on the plunging point in case of plunging breakers, or the intermediate point between lines 1 and 3 for spilling breakers. From the third line, the measuring lines were arranged in the inner regions where the surface rollers developed well. The lowest measuring points in each measuring line are 1mm above the bottom in case of 1/20 slope, and for the cases of 1/30 slope they are 2mm above the bottom. The vertical distance of those points were 1-20mm and the highest points are near the mean water levels. For example, the arrangement of Case 1 is shown in Fig.1.

In Case 5, the measuring points were taken only close to the bottom to investigate the detail of the bottom boundary layer in the surf zone. Nine measuring lines were allocated every 40cm of distance from the offshore side of the breaking point to the still water shoreline. The measuring points were arranged 1, 2, 3, 5, 10 and 20mm above the bottom along each line.

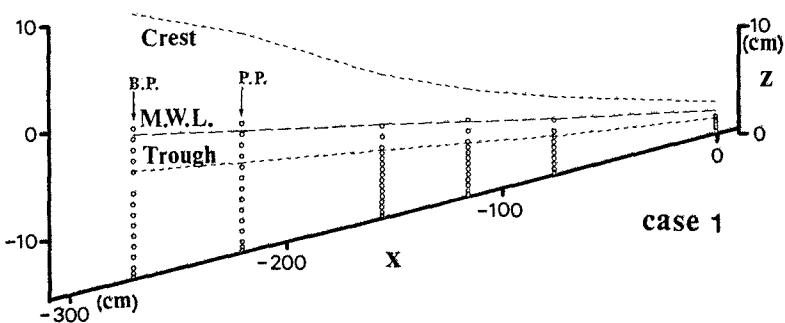


Fig.1 Arrangement of the measuring points for Case 1.

## 2.2 Data Processing and Analysis

A two-component laser doppler velocimeter was used to measure the time history of two-dimensional velocity vector lying on the  $xz$ -plane. The velocity data were sampled every 10ms and were converted into digital data over 100 wave periods. The data of the water surface elevation over the measuring point were also taken simultaneously by using a capacitance-type wave gage.

The ensemble mean (equi-phase-mean) value of velocity which is expressed by  $u$  in  $x$ -direction or  $w$  in  $z$ -direction was calculated as the average of the velocity at the same phase of every wave. The steady current was calculated from those ensemble mean values. The turbulence component denoted by  $u'$  or  $w'$  was determined as the deviation from the ensemble mean value. The Reynolds stress was calculated from the turbulence. The mean Reynolds stress  $-\rho\overline{u'w'}$  was obtained by averaging the Reynolds stress over one wave period, where  $\rho$  is the water density. From the steady current and the mean Reynolds stress, the mean eddy viscosity coefficient  $\nu_t$  was calculated by using the eddy viscosity model.

## 2.3 Experimental Results

Figure 2 gives an example of the steady current distribution for Case 2. It can be seen that the undertow profile in the inner region is significantly different from that around the breaking point. Figure 3 is the steady current of Case 5. In the inner region the velocity at the elevation of 1mm above the bottom indicates large value in the offshore direction, while it still directs onshore at the plunging point. This is because the oscillatory bottom boundary layer in the inner region does not develop well due to the agitation of the turbulence from the upper layer. The

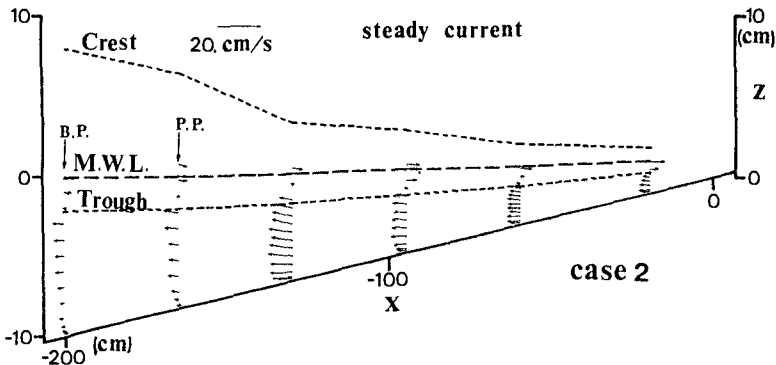


Fig.2 Distribution of the steady currents for Case 2.

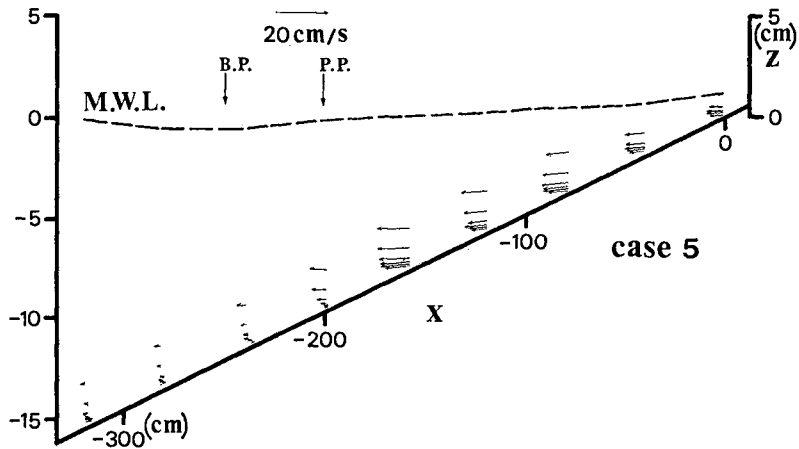


Fig.3 Distribution of the steady currents for Case 5.

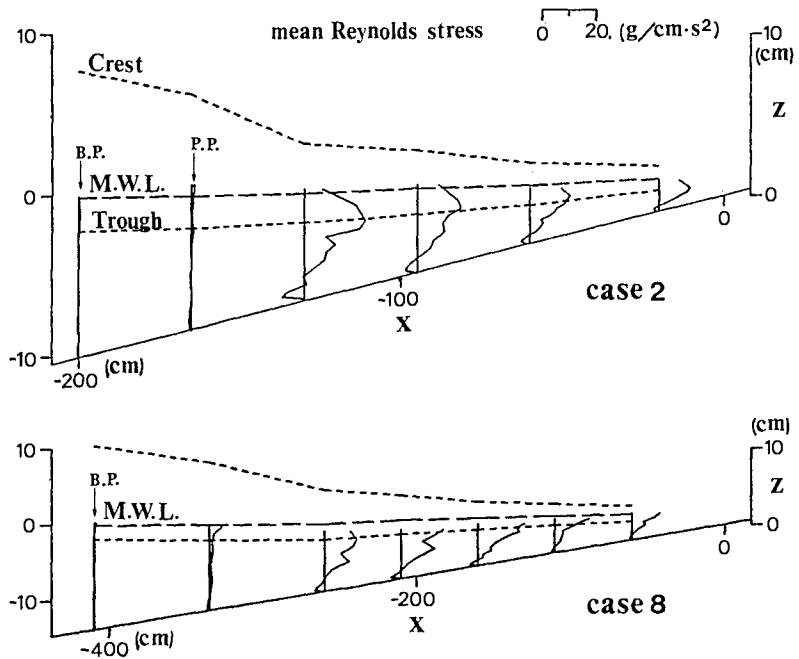


Fig.4 Distributions of the mean Reynolds stress for Cases 2 and 8.

influence by the bottom to the steady current can be seen up to 3mm above the bottom there.

Figure 4 shows the distributions of the mean Reynolds stress of Cases 2 and 8. The distributions of the mean eddy viscosity coefficient of those cases are given in Fig.5. In the figures, it can be seen that both of them decrease linearly from the trough level to the bottom in the inner region. On the bottom, the value of the mean eddy viscosity coefficient is very small compared with that at the trough level. This should corresponds to the fact that the turbulence produced by the large vortex on the front face of the wave crests is far larger than that generated near the bottom. But with respect to the mean Reynolds stress, it is observed that the offshoreward directed shear stress is too large to be neglected. Some researches were done with the assumption that the mean eddy viscosity is independent of the vertical coordinate [ e.g. Svendsen and Hansen (1988) or Tsuchiya et al.(1988) ], but the result of this study is not consistent with that assumption.

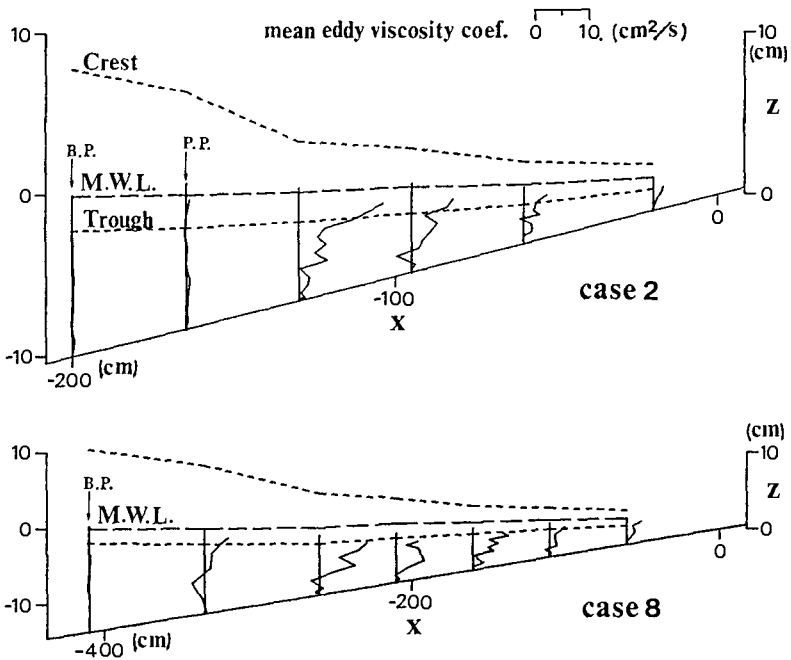


Fig.5 Distributions of the mean eddy viscosity coefficient for Cases 2 and 8.

## 3 MODELING OF UNDERTOW

## 3.1 On-offshore Variation of Vertically Averaged Undertow

It can be considered that the mass flux by the breaking waves in the inner region consists of two components, the mass flux by the wave motion and that by the large vortex formed just in front of the wave crest. That means, the vertically averaged value of the undertow can be separated into two parts which are the contribution  $U_S$  from the wave component and  $U_r$  from the onshore mass flux by the large vortex [Okayasu et al.(1986)].

$U_S$  can be calculated from the wave profile by using the stream function method of Dean (1965). As the calculation by the stream function method is done with the assumption of no shear stress on the bottom, the velocity very close to the bottom should not agree with the actual velocity. However, it would not be a problem when we discuss about the vertically averaged on-offshore steady current because the oscillatory bottom boundary layer by the wave motion is much thinner than that of the steady current.

On the other hand,  $U_r$  in the inner region can be estimated by the square of the local wave height  $H$  as Svendsen (1984) did, and it does not depend on the incident wave condition. The onshore mass flux by the large vortex can be expressed as

$$M_r = \frac{AH^2}{T} , \quad (1)$$

where  $A$  is a constant. And  $U_r$  can be obtained by dividing  $M_r$  by the trough level  $d_t$  as

$$U_r = - \frac{AH^2}{d_t T} . \quad (2)$$

The calculated value  $U_c$  of the vertically averaged undertow in the inner region is

$$U_c = U_S + U_r = U_S - \frac{AH^2}{d_t T} . \quad (3)$$

In the equation, we used the value

$$A = 2.3 , \quad (4)$$

in all cases based on the laboratory data. In order to decide  $A$ , the value

$$A' = - ( U_m - U_S ) \frac{d_t T}{H^2} , \quad (5)$$

was calculated for each measuring line except Case 5, where  $U_m$  is the vertically averaged value of the measured undertow. Next we averaged  $A'$  of all measuring lines in the inner region, and took the average again for all cases. The influence of the bottom slope to the constant  $A$  could not be

revealed by the experiments.

The comparison between the calculated value  $U_c$  and measured value  $U_m$  for Case 2 is shown in Fig.6. Here we set  $A$  equal to be 0 from the breaking point to the plunging point then changed the value linearly in the distance to the inner region. The value  $A$  was 2.3 in the inner region.

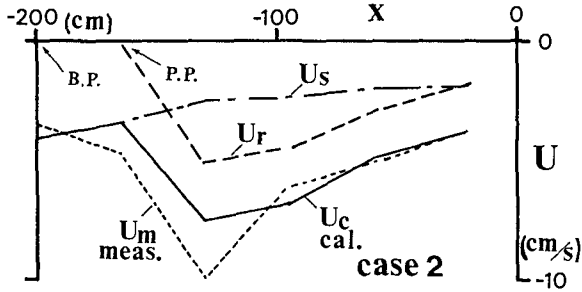


Fig.6 Comparison between the measured and the calculated value of the vertically averaged undertow for Case 2.

3.2 Modeling of Vertical Distributions of Mean Reynolds Stress and Mean Eddy Viscosity

Based on the experimental results mentioned in Section 2.3, the vertical distributions of the mean Reynolds stress and the mean eddy viscosity coefficient can be assumed as linear functions of the vertical elevation  $z$ . This assumption is different from that used by Svendsen and Hansen (1988) or Tsuchiya et al.(1988). Figure 7 shows this

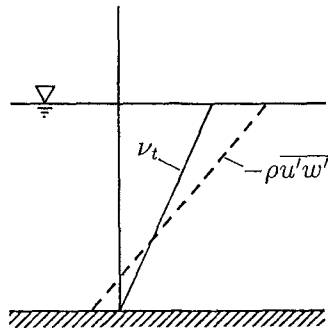


Fig.7 Assumed distributions of the mean Reynolds stress and the mean eddy viscosity coefficient.

model. The constants in the model were investigated as follows.

First, the coefficients of the linear functions for the measuring lines 4 and 5 were obtained for all cases by using the regression analysis. Then the coefficients were non-dimensionalized by using the water density  $\rho$ , the celerity  $c$  and the trough depth  $d_t$  as the representative values. At last, the averages of the measuring lines 4 and 5 were taken. Using these parameters, the linear functions was expressed as

$$-\rho \overline{u^T w^T} = \alpha_1 \rho \frac{c^2}{d_t} z' + \beta_1 \rho c^2, \quad (6)$$

$$v_t = \alpha_2 c z' + \beta_2 c d_t, \quad (7)$$

where  $\alpha_1$ ,  $\beta_1$ ,  $\alpha_2$  and  $\beta_2$  are dimensionless parameters and  $z'$  is the vertical elevation from the bottom. The wave celerity is expressed as

$$c = \sqrt{g (d_t + H)}, \quad (8)$$

on the basis of the solitary wave theory, where  $g$  is the gravity acceleration. Table 2 is the list of the dimensionless parameters.

Table 2 Dimensionless parameters for the distribution of  $-\rho \overline{u^T w^T}$  and  $v_t$

Case	slope	$\alpha_1$	$\beta_1$	$\alpha_2$	$\beta_2$	$\gamma_2$
1		0.0024	-0.00058	0.015	-0.00042	0.015
2		0.0027	-0.00062	0.015	-0.0015	0.014
3	1/20	0.0020	-0.00026	0.0098	0.0013	0.011
4		0.0022	-0.00016	0.015	0.0015	0.016
Ave. of 1/20		0.0023	-0.00041	0.014	0.00022	0.014
6		0.0018	-0.00036	0.010	0.000066	0.010
7		0.0015	-0.00024	0.017	-0.00052	0.016
8	1/30	0.0019	-0.00036	0.011	-0.00043	0.010
9		0.0013	-0.00024	0.0091	-0.00010	0.0081
10		0.0011	-0.00016	0.0046	0.00042	0.0050
Ave. of 1/30		0.0015	-0.00027	0.010	-0.00011	0.0099

In the table, the parameter  $\beta_2$  is the dimensionless value of  $v_t$  on the bottom ( $z' = 0$ ) and  $\gamma_2$  is the value at the trough level ( $z' = d_t$ ). We can find that  $\beta_2$  is far smaller than  $\gamma_2$  and it is consistent with the experimental result. Therefore, it should be possible to take  $v_t = 0$  on the bottom. Equation (7) can be approximated as

$$v_t = \alpha_2 c z'. \quad (9)$$

In each bottom slope, the variance of the parameters is so small that the parameters can be regarded as constants. Hence the averaged values are taken for each slope.

Considering the influence of the bottom slope  $\tan\beta$ , we simply express the parameters as

$$\begin{aligned}\alpha_1 &= 0.046 \tan\beta , \\ \beta_1 &= -0.008 \tan\beta , \\ \alpha_2 &= 0.30 \tan\beta .\end{aligned}\tag{10}$$

Substituting Eq.(10) into Eqs.(6) and (9), we obtain the equations for the distributions of the mean Reynolds stress and the mean eddy viscosity coefficient as

$$-\rho \overline{u'w'} = 0.046 \tan\beta \rho \frac{c^2}{d_t} z' - 0.008 \tan\beta \rho c^2 ,\tag{11}$$

$$v_t = 0.30 \tan\beta c z' .\tag{12}$$

### 3.4 Vertical Variation of Undertow

By using the eddy viscosity model, the relation between the mean shear stress  $\bar{\tau}$  acting on the horizontal plane and the steady current  $U$  in  $x$ -direction is expressed as

$$\bar{\tau} = \rho v_t \frac{\partial U}{\partial z} .\tag{13}$$

Transforming  $\bar{\tau}$  to  $-\rho \overline{u'w'}$  and considering Eq.(6), we obtain the equation

$$\frac{1}{\rho} \frac{\partial \bar{\tau}}{\partial z} = \frac{\partial}{\partial z} \left[ v_t \frac{\partial U}{\partial z} \right] \equiv C_1 ,\tag{14}$$

where  $C_1$  is a constant. And from the Eq.(9),  $v_t$  can be expressed as

$$v_t = C_2 z' ,\tag{15}$$

where  $C_2$  is also a constant. If using  $z'$  instead of  $z$ , we get

$$\frac{\partial}{\partial z'} \left[ z' \frac{\partial U}{\partial z'} \right] = \frac{C_1}{C_2} ,\tag{16}$$

from Eq.(14). This equation can be integrated by using integral constants  $C_3$  and  $C_4$  as

$$U = C_3 \ln z' + C_4 + \frac{C_1}{C_2} z' .\tag{17}$$

It can be considered that the third term of the right hand side of Eq.(17) directly expresses the "shear effect" termed by Nadaoka and Hirose (1986).  $C_1$  and  $C_2$  can be decided as

$$C_1 = 0.046 \tan\beta \frac{c^2}{d_t} ,\tag{18}$$

$$C_2 = 0.30 \tan\beta c ,\tag{19}$$

from Eqs.(11) and (12). The boundary condition at the trough level is given by using Eq.(13) as

$$\left. \frac{\partial U}{\partial z'} \right|_{d_t} = \frac{1}{\rho} \left. \frac{\bar{\tau}}{v_t} \right|_{d_t} = \frac{0.038 \tan \beta c^2}{C_2 d_t} . \quad (20)$$

Substituting Eq.(20) into the first derivation of Eq.(17) which is

$$\frac{\partial U}{\partial z'} = \frac{C_3}{z'} + \frac{C_1}{C_2} , \quad (21)$$

we obtain

$$C_3 = \left[ \frac{0.038 \tan \beta c^2}{C_2 d_t} - \frac{C_1}{C_2} \right] d_t = -0.027c . \quad (22)$$

Furthermore, By using the relation

$$\begin{aligned} U_c &= \frac{1}{d_t} \int_0^{d_t} U dz' \\ &= C_3 ( \ln d_t - 1 ) + C_4 + \frac{1}{2} \frac{C_1}{C_2} d_t , \end{aligned} \quad (23)$$

the constant  $C_4$  is given as

$$C_4 = U_c + C_3 ( 1 - \ln d_t ) - \frac{1}{2} \frac{C_1}{C_2} d_t . \quad (24)$$

From the equations above, the vertical distribution of the undertow can be obtained as

$$\begin{aligned} U &= U_c + C_3 \left( \ln \frac{z'}{d_t} + 1 \right) + \frac{C_1}{C_2} \left( z' - \frac{d_t}{2} \right) \\ &= -0.027c \ln \frac{z'}{d_t} + 0.15c \frac{z'}{d_t} - 0.10c + U_c . \end{aligned} \quad (25)$$

In the equation, the bottom steepness  $\tan \beta$  does not appear.

#### 4. COMPARISONS WITH THE EXPERIMENTAL RESULTS

Using Eq.(25), we can evaluate the undertow profile from the time history of the wave profile at that point. Figure 8 gives the comparisons between the measured and the calculated undertow profiles for the measuring lines 3 and 5 of 1/20 slope by using Eq.(25). In the figure, a dimensionless value which is obtained by dividing  $U$  by the absolute value of  $U_c$  is taken for the horizontal coordinate, and the vertical coordinate is  $z'/d_t$ . The positions of the measuring lines are indicated by  $x/x_b$ . The comparisons for the 1/30 slope are also shown in Fig.9.

The nondimensional parameters which determine the each constant in Eq.(25) are invariant through the all cases and

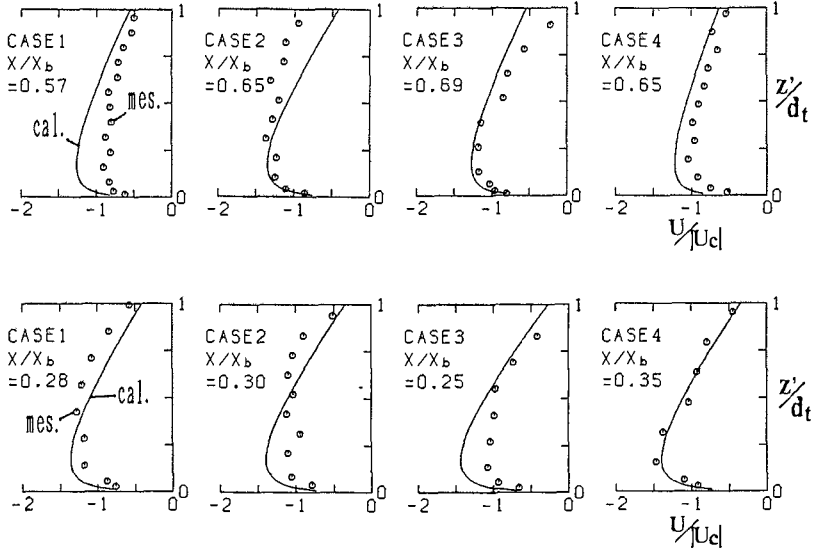


Fig.8 Comparisons between the measured and the calculated undertow profiles for the 1/20 slope.

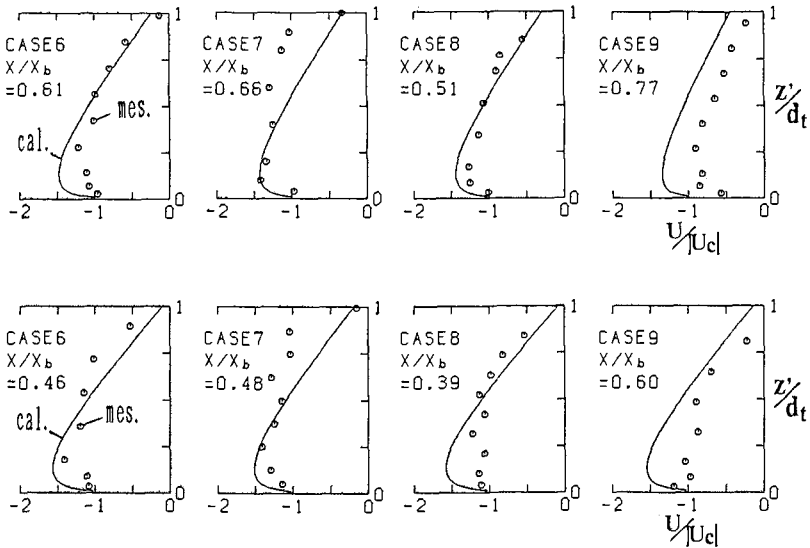


Fig.9 Comparisons between the measured and the calculated undertow profiles for the 1/30 slope.

the agreement between the measured and calculated values is good. However, in general the gradient of the calculated values are a little smaller than the measured values in the upper regions, that means the further investigation for estimating  $C_1$  and  $C_2$  in Eq.(25) is required.

Figure 10 shows the comparisons when we apply Eq.(25) to Case 5 of the 1/20 slope. The agreement is well especially in the area close to the bottom. It can be said that the model is usable for evaluating the steady current distribution close to the bottom in various conditions.

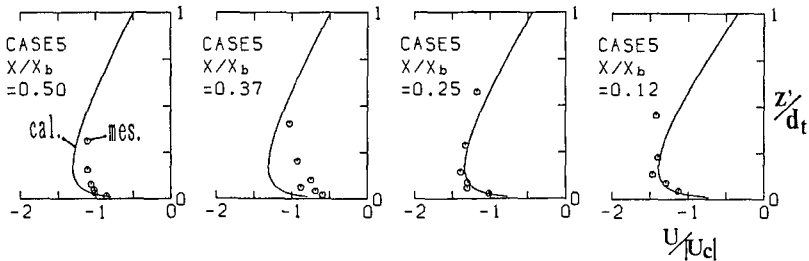


Fig.10 Comparisons between the measured and the calculated undertow profiles for Case 5.

## 5. CONCLUDING REMARKS

The velocity distribution in the surf zone on 1/20 and 1/30 constant slopes was measured in detail by using a two-component laser doppler velocimeter. The distributions of the steady current, the mean Reynolds stress and the mean eddy viscosity coefficient were evaluated. A model was proposed to estimate the vertical distribution of the undertow in the inner region, especially close to the bottom.

The conclusions are as follows.

(1) The mean Reynolds stress and the mean eddy viscosity coefficient in the inner region can be regarded as linear functions of the vertical elevation. The offshore directed mean shear stress on the bottom is so large that it can not be neglected. The nondimensional parameters which express the linear distribution can be expressed in terms of the bottom slope.

(2) The vertically averaged on-offshore steady current can be evaluated from the sum of two components: the first component is resulted from the wave component and the second one from the large vortex formed just in front of the wave crest. The second component can be evaluated by the square of the local wave height.

(3) The vertical distribution of the undertow in the inner region of the surf zone can be estimated by using Eq.(25). The calculated undertow profiles agree well with the measured values near the bottom. However, further investigations are required for the accurate evaluation around the trough level.

## REFERENCES

- Bagnold, R.A. (1940) : Beach formation by waves; some model experiments in a wave tank. *J. Institute Civil Eng.*, Vol.15, pp.27-52.
- Dean, R.G. (1965) : Stream function representation of nonlinear ocean wave, *J. Geophysical Res.*, Vol.70, No.18, pp.4561-4572.
- Hansen, J.B. and I.A. Svendsen (1984) : A theoretical and experimental study of undertow, *Proc. 19th ICCE.*, pp.2246-2262.
- Nadaoka, K. and F. Hirose (1986) : A modeling of water particle dispersion under breaking waves in the surf zone, *Proc. 33rd Japanese Conf. Coastal Eng.*, pp.26-30. (in Japanese)
- Okayasu, A., T. Shibayama and N. Mimura (1986) : Velocity field under plunging waves, *Proc. of 20th ICCE.*, pp.660-674.
- Svendsen, I.A. (1984) : Mass flux and undertow in a surf zone, *Coastal Eng.*, Vol.8, pp.347-365
- Svendsen, I.A. and J.B. Hansen (1988) : Cross-shore currents in surf zone modeling, *Coastal Eng.*, Vol.12, pp.23-42.
- Tsuchiya, Y., T. Yamashita and M. Uemoto (1988) : A model of undertow in the surf zone, *Coastal Eng. in Japan*, Vol.30, No.2, pp.63-73.